Matter-wave diffraction of quantum magical helium clusters

Oleg Kornilov * and J. Peter Toennies,
Max-Planck-Institut für Dynamik und Selbstorganisation, Bunsenstraße 10 • D-37073 Göttingen • Germany.
* Present address: Chemical Sciences Division, Lawrence Berkeley National Lab., University of California • Berkeley, CA 94720 • USA.
DOI: 10.1051/epn:2007003

Back in 1868 the element helium was discovered in and named after the sun (Gr. "helios"), an extremely hot environment with temperatures of millions of degrees. Ironically today helium has become one of the prime objects of condensed matter research at temperatures down to 10^{-6} Kelvin. With its two very tightly bound electrons in a 1S shell it is virtually inaccessible to lasers and does not have any chemistry. It is the only substance which remains liquid down to 0 Kelvin. Moreover, owing to its light weight and very weak van der Waals interaction, helium is the only liquid to exhibit one of the most striking macroscopic quantum effects: superfluidity. First recognized in 1938 by Pyotr Kapitza (Nobel prize 1978) the many macroscopic manifestations of superfluid behavior have over the last 70 years garnered a tremendous theoretical effort, but even today the statement made some years ago still holds "the explicit connection between superfluidity and Bose Einstein Condensation is not trivial" [1].

Small clusters of helium atoms, the subject of this report, also show a number of strange magic-like quantum properties not found in any of the other many clusters under investigation. For example, the existence of the helium dimer, which has long served as an important model system for quantum chemistry, was questioned up to about 10 years ago. The problem was that even minute energetic differences decide on whether the dimer has a bound state. In 1993 the first published claim of its detection in a molecular beam of clusters using a mass spectrometer met with skepticism because of the complications arising from extensive fragmentation following electron impact ionization. The existence of the helium dimer was finally established in 1994 when our group was able to detect the matter-wave diffraction of He dimers from a nanostructured transmission grating [2].

The properties of larger helium clusters are of great interest for nuclear many-body theoreticians because of the many close analogies between nuclei and helium clusters. Helium atoms have the advantage over nucleons, that their interactions depend only on the interatomic distance and do not involve complicated tensorial terms.

Finally, helium clusters are the only clusters which are definitely liquid. This property led to the development of a new experimental technique of inserting foreign molecules into large helium clusters, which serve as ultra-cold nano-containers. The virtually unhindered rotations of the trapped molecules as indicated by their sharp clearly resolved spectral lines in the infrared has been shown to be a new *microscopic* manifestation of superfluidity [3], thus linking cluster properties back to the bulk behavior of liquid helium.

Today one of the aims of modern helium cluster research is to uncover the secrets of superfluidity by a bottom-up approach, starting from the smallest cluster, the dimer, and proceeding on to larger clusters with more than 50 atoms. And indeed our experiments have uncovered a number of new bizarre and magic quantum phenomena at all sizes as is discussed in the following sections.

Matter-Wave Diffraction as a Non-destructive Mass Spectrometer

The break-through in establishing the existence of the dimer derives from the fact that diffraction depends only on the de Broglie wavelengths of the particles passing *through* the slits and therefore allows for the *non-destructive* analysis of the clusters in a molecular beam. Atom beam diffraction had been demonstrated in 1988 by David Pritchard and his group at MIT, but their apparatus was limited to alkali atoms and dimers, which can be converted with near 100 % efficiency into ions when they strike a hot tungsten wire. Helium atoms and their clusters can only be detected by the much less efficient process of electron impact ionisation.

An overview of our cluster beam apparatus is shown in Fig.1. The clusters are produced in a cryogenic free jet expansion of helium gas at a temperature $T_0 \leq 100K$ and $P_0 \approx$ 1-100 bar pressures into a high vacuum. They grow in size in the course of the dramatic cooling accompanying the adiabatic expansion. The heart of the apparatus is the free standing SiN_x grating (Fig.2) with an exact period of 99.90 ± 0.05 *nm* and typically 50 % transmission through the slits, which are only 50 *nm* wide. Similar gratings were first fabricated in 1995 in the group of Prof. Hank Smith at MIT by his student Tim Savas. This was a remarkable technological achievement since even today more than 10 years later, despite the spectacular advances in nanotechnology, it has not been possible to reduce the dimensions of *free standing* structures.

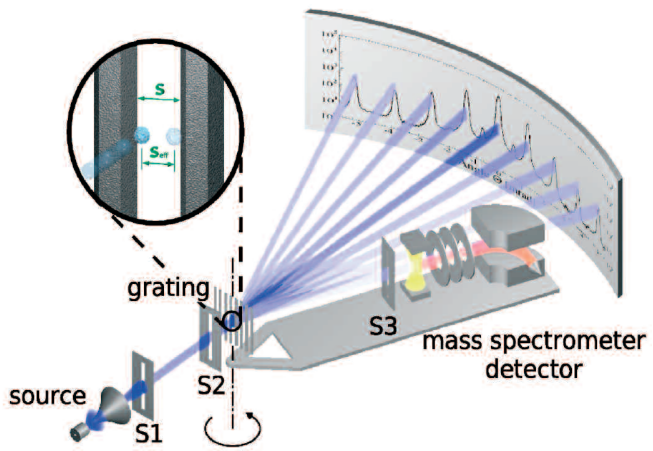

◀ **Fig. 1:** Schematic diagram of the cluster beam apparatus used for the diffraction of small He clusters. The entire apparatus is divided up into several vacuum compartments (not shown). The mass spectrometer detector is operated in an ultrahigh vacuum of 10^{-11} mbar to suppress the residual gas background. The inset illustrates the interaction of the clusters with the grating bars and the resulting reduction in slit width.

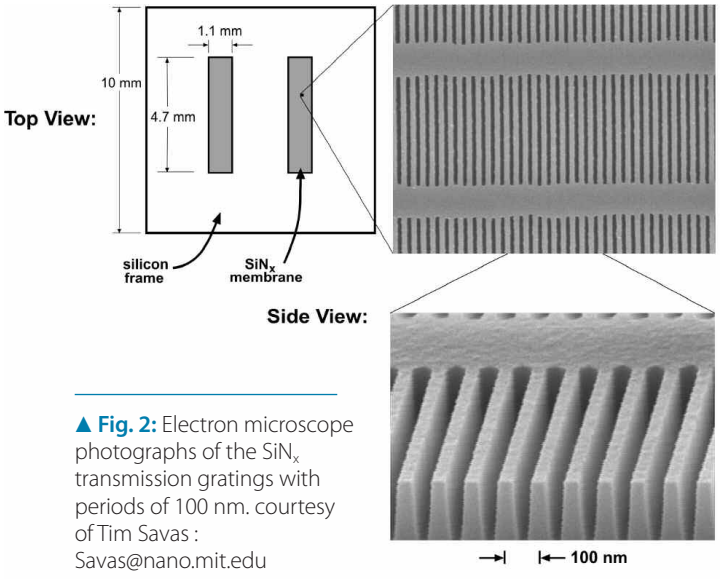

▲ **Fig. 2:** Electron microscope photographs of the SiN_x transmission gratings with periods of 100 nm. courtesy of Tim Savas : Savas@nano.mit.edu

According to Louis de Broglie all moving particles have a wavelength λ, which is inversely proportional to their translational momentum,

$$\lambda = \frac{h}{M \cdot v} \qquad (1)$$

where M is the particle mass. In the case of helium clusters $M = N \cdot m$, where m is the mass of one atom. The diffraction angles are then given by

$$\theta \cong n\frac{\lambda}{d} = \frac{h}{dNmv}, \qquad (2)$$

where n is the diffraction order. Since the clusters all have the same velocities the diffraction angles are inversely proportional to N, the number of atoms in the cluster. In complete analogy to an optical grating spectrograph each cluster is expected to appear at a diffraction angle depending only on its number size.

Fig.3 shows a series of diffraction patterns for a room temperature source (T_0 = 300 K) and decreasing source temperatures T_0 = 60, 24 and 6K. Especially noteworthy is the huge range in the detected signals over four orders of magnitude which makes it possible to detect a large number of diffraction orders. This was a delightful surprise, not envisaged when we first contemplated these experiments. According to Eq.(2) the peaks at angles halfway between the dominant monomer peaks at T_0 = 60, 24, and 6 K can be assigned to the helium dimer (see especially Fig 3(e)). Additional structures at smaller angles seen at T_0 = 6 K are due to the trimer and larger clusters, to be discussed later. Our 1994 experiments and subsequent studies provided the first unequivocal experimental evidence for the existence not only of the helium dimer, but also of the trimer, tetramer and larger clusters.

The excellent resolution in these experiments is made possible by the inherently sharp velocity distributions $\Delta v/v \sim 1\%$ of He beams produced in free jet expansions from 5 μm dia pin holes. This feature and the narrow (~10 μm) collimating slits S1 and S2 (Fig.1) provide for large wave packets with longitudinal and transverse coherence lengths of 10 nm x 20 μm, respectively. Fortunately the small clusters in free jet expansions have the same sharp velocities as the atoms, which are typically $v \cong 200 - 300 m$/sec depending on the source temperature. Another important feature of the apparatus is a stable construction to allow an angular reproducibility of the order of 10^{-6} rad. The detection of low signals of only 1 count/s of either the He^+ or He_2^+ fragments is facilitated by the inherently low background on these masses in ultra-high vacuum chambers, the basis for the ubiquitous helium leak detector used by vacuum experimentalists.

The diffraction technique has been used to discover and identify a number of other unusual clusters. Small $^4He_m{}^3He_n$ clusters have attracted considerable attention from theorists because of spin pairing of the fermionic ^{3}He atom constituents. Altogether 11 tenuous complexes including the three-body halo molecule $^4He_2{}^3He$ and the pseudo-Borromean complex $^4He_2{}^3He_2$ could be identified by diffraction [4]. The diffraction experiments have also been applied to mixed HeH_2 dimers as well as H_2 and D_2 clusters. Unfortunately it has not been possible to produce small pure clusters of ^{3}He with less than about 500 atoms which are predicted to exhibit striking shell-closing effects, like the electrons in an atom, leading to magic number stabilities. The interatomic potentials are the same as in ^{4}He, but the smaller mass rules out a bound dimer. The smallest stable cluster, according to the most recent calculations, consists of 32 atoms. Thus the detection of small ^{3}He clusters remains a challenge for future work.

These experiments illustrate the advantages of the diffraction method. It does not suffer from the ambiguities resulting from fragmentation in a mass spectrometer since the diffraction experiment appeals only to the wave nature of those clusters which pass through the slits without an appreciable phase shift. The size analysis takes full advantage of *wave-particle duality* so that even the most weakly bound species can be detected. This technique opened up a vast new field of neutral particle non-destructive mass analysis.

Measurements of Cluster Properties via Matter-Wave Diffraction

The intensities of the diffraction peaks provide information on the interactions of the particles with the grating bars as well as the geometrical sizes of the clusters. As is well known from the analogy to optics the distribution of the peak intensities over various diffraction orders is given by the "slit function", which is the same as the Fraunhofer pattern for diffraction from a single slit. Thus the angular halfwidth of the envelope of the peak height distribution is given by $\Delta\theta = 0.88\,\frac{\lambda}{S_{eff}}$, where S_{eff} is the effective width of a single grating slit. Experiments with different rare gases He, Ne, Ar, Kr and D_2 reveal intensity patterns which are modified by the van der Waals interaction with the grating bars, which causes a reduction in the effective slit width. This led to the first determination of the van der Waals coefficients for ground state rare gas and Na atoms [5] and electronically excited metastable atoms [6].

Large differences are also found between the slit function of He atoms and that of the dimers which are best seen at T_0 = 6 K (Fig.3(d)). As illustrated in the inset of Fig. 1, dimers which come too close to the bars will break up and their effective slit width is reduced by ½ $\langle R \rangle$, where $\langle R \rangle$ is the expectation value of the interatomic distance of the two atoms in the dimer (see Eq.(B5) in the box) a result which agrees with a rigorous three-body scattering theory. The size of the dimer determined in this way from data similar to Fig. 3 (d) is $\langle R \rangle = 5.2 \pm 0.4\ nm$ [7]. The extraordinary size of the dimer can be appreciated by comparing it with the H_2 molecule for which $\langle R \rangle = 0.074\ nm$. We even go so far as to claim that the helium dimer is the largest naturally occuring ground state molecule in the universe. Since its average interatomic distance is about 3.5 times larger than its classical outer turning point the molecule exists mostly in the classically ···

••• forbidden region of space, a property which in Nuclear Physics is referred to as a halo state. This large size of the dimer has the bizarre effect on scattering from a gas of Kr atoms that the Kr atoms collide in 98% of the collisions with either one or the other of the He atoms (see Eq.(B6)) and can even pass between the two He atoms without breaking the bond [8].

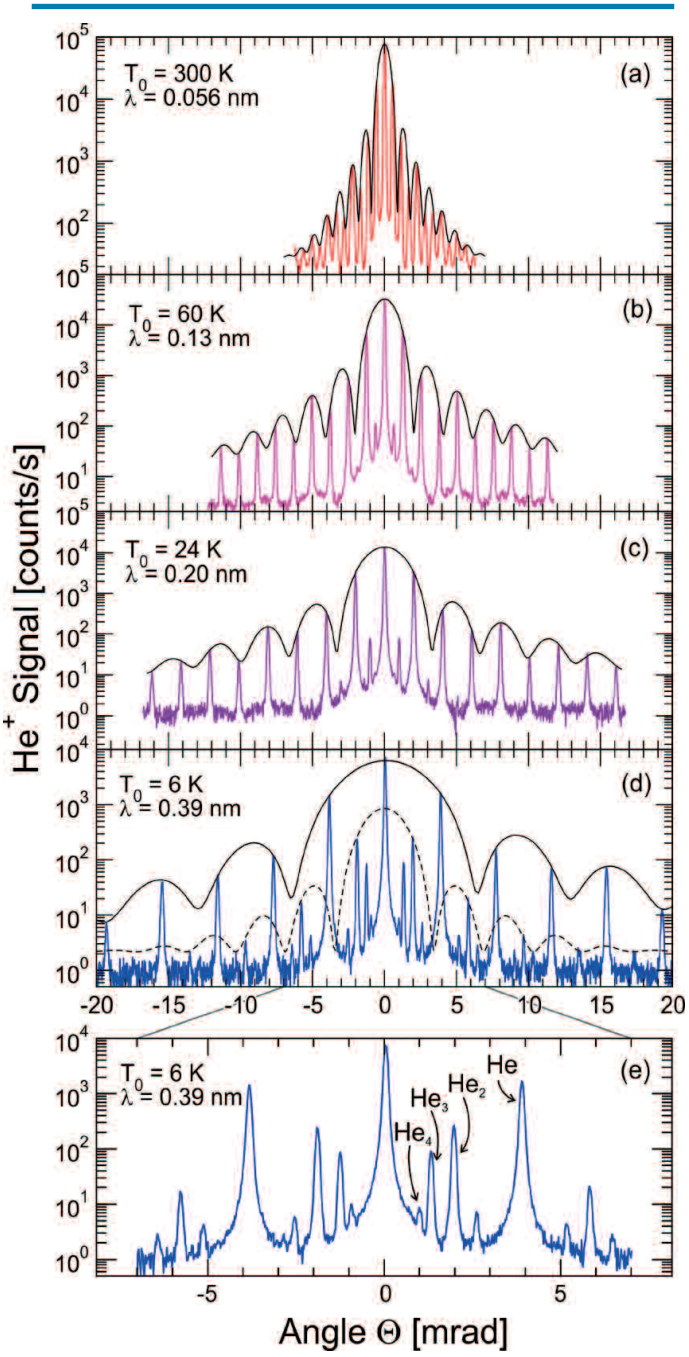

▲ **Fig. 3:** (a) to (d): Diffraction patterns measured for different source temperatures at source pressures ranging from 150 to 1.5 bar (top to bottom). The major peaks are from helium atoms and have been fitted to the corresponding slit functions (solid line curves). Dimers are seen half way between the first order atom peaks at θ_1, for $T_0 \leq 60$ K. The dimer slit function fitted to the dimer peaks up to n = 9 at $T_0 \leq 6$ K is shown by the dashed curve. (e): Trimers (1/3 θ_1) and tetramers (1/4 θ_1) are also clearly resolved at $T_0 \leq 6$ K.

The theory of halo states (Eq.(B3)) also makes it possible to calculate from $\langle R \rangle$ the binding energy of the dimer to be $E_b = 1.3 \cdot 10^{-3} K (1.1 \cdot 10^{-7} eV)$. In view of its weak binding it became clear that the dimer has only a ground vibrational state, and no rotational states other than the ground state j = 0, making it a spherical molecule. Fig.4(a) shows the radial density distribution

Box: Quantum Two-Body Halo states

The He dimer and possibly $^3He(H_2)$ are the only known molecular analogs of the halo state of the deuteron. Two- and also many-body halo states have been observed in a number of other nuclei. Halo systems are described in first order approximation by neglecting the inner potential. This is justified by the large extent of the wave function into the classically forbidden region $R > R_{out}$, where R_{out} is the outer classical turning point. There the radial wave function is given by

$$\varphi(R) \rightarrow \frac{e^{-kR}}{R}, for\ R > R_{out} \qquad \text{(B1)}$$

where $k = \sqrt{2\mu E_b}/\hbar$, and μ is the reduced mass and E_b, the binding energy. The average radius is easily calculated

$$< R > = \frac{4\pi \int_0^\infty R \frac{e^{-2kR}}{R^2} \cdot R^2 dR}{4\pi \int_0^\infty \frac{e^{-2kR}}{R^2} \cdot R^2 dR} = \frac{1}{2k} \qquad \text{(B2)}$$

and therefore

$$< R >^2 = \hbar^2 (8\mu E_b)^{-1} \qquad \text{(B3)}$$

The projection of along a Cartesian coo rdinate in a direction perpendicular to the grating bars is given by

$$\langle X \rangle = \frac{\iint |X| \sin\vartheta \, d\vartheta \, d\phi}{\iint \sin\vartheta \, d\vartheta \, d\phi} = \frac{1}{2} \langle R \rangle \qquad \text{(B4)}$$

where $|X| = \langle R \rangle \sin\vartheta |\cos\phi|$. Thus the reduction in slit width due to the finite size of the dimer is

$$S_0 - S_{eff} = \frac{1}{2} \langle R \rangle \qquad \text{(B5)}$$

The large size of a halo system also affects its interactions with other particles as first pointed out by Roy Glauber in 1955 [15]. According to Glauber the neutron and proton in the deuteron are so far apart that other nucleons or π-mesons will only be scattered from either of the constituents except when one lies in the shadow of the other causing an eclipse. Thus the classical cross section is given by

$$\sigma_2 = 2\sigma - \frac{\sigma_1^2}{4\pi \langle R \rangle^2} \qquad \text{(B6)}$$

where σ_1 and σ_2 denote the cross sections for scattering from the halo, or one of its constituents, respectively. The second term on the right is the eclipse correction. This effect has recently been found for the He dimer in scattering from Kr atoms [8] for which the eclipse correction amounts to only 2 %. Thus in 98 % of the collisions the Kr atom interacts only with one of the He atoms, implying, moreover, that it can pass between the He atoms without breaking the dimer bond!

of the two bound atoms in the dimer. From the scattering length, given by $\alpha = 2\langle R\rangle = 10.4\ nm$, the asymptotic ($T \to 0$) total scattering cross section can be calculated to be $\sigma = 8\pi\alpha^2 = 2{,}720\ \mathrm{nm}^2$. Thus the enormous size of the dimer, its miniscule binding energy, and the gigantic He-He scattering cross section are all manifestations of its small mass and weak binding.

Table I compares the ground state helium dimer with the electronically excited dimer, which correlates asymptotically to the 2 $^3S_1$ and 2 $^3P_0$ states, and with the sodium dimer in a highly excited vibrational state. In Table I it is interesting to note the remarkable physical similarities between the halo state of the deuteron and that of the He dimer. Of course the deuteron is more tightly bound by a factor 10^{13} in the energy but is smaller in size by 6 orders of magnitude (Table I), which is consistent with Eq.(B3).

These dimer results also provide a discriminatory test of quantum chemical calculations of the van der Waals potential between two He atoms, one of the most important benchmarks for accurate calculations. The giant He-He cross section also explains the extremely low temperatures ($\approx 10^{-3} K$) in He atom free jet expansions widely used as a medium for cooling large molecules to facilitate their high resolution spectroscopic investigations. And, of course, a precise He-He potential curve is needed for understanding the many unique properties of the bulk liquid, including its superfluidity, as well as the unusual properties of the solid.

The size of the trimer has also recently been measured using the same method described above [11]. As proposed by Lim and coworkers in 1977 the He trimer is the only naturally occurring three-body system presently expected to exhibit an exotic quantum state, first predicted in 1970 by the Russian nuclear theorist Vitali Efimov. Efimov pointed out that if the binding between any two of three identical bosons is critical, *i.e.* if $E_b = 0$, and $a = \infty$, then the three-body system would have an infinite number of bound states. As opposed to ordinary bound states, however, the Efimov states disappear when the strength of the two-body potential is *increased*. Thus these states only exist in extremely weakly bound and, in fact, even for very slightly *unbound* systems. Despite many searches a three-body Efimov state has not been found in nuclear systems. Recent calculations predict a huge average distance between the individual atoms for the first excited Efimov state of $< r > = 0.96\ nm$. The average distance between the atoms in the ground state, although much smaller, still is quite large and equals. The measurements of the trimer slit function yield an average bond distance in the trimer of $< r > = 1.^{+0,4}_{-0,5}\ nm$ [11]. With the concentration of Efimov trimers estimated to be about 10 % the expected concentration-weighted average bond distance comes to $< r > = 1.7\ nm$, which is 0.2 *nm* larger than the experimental upper limit of 1.5 nm. Thus this experiment could not convincingly confirm the existence of the excited Efimov state of the $^4He_3$ with the size predicted by theory.

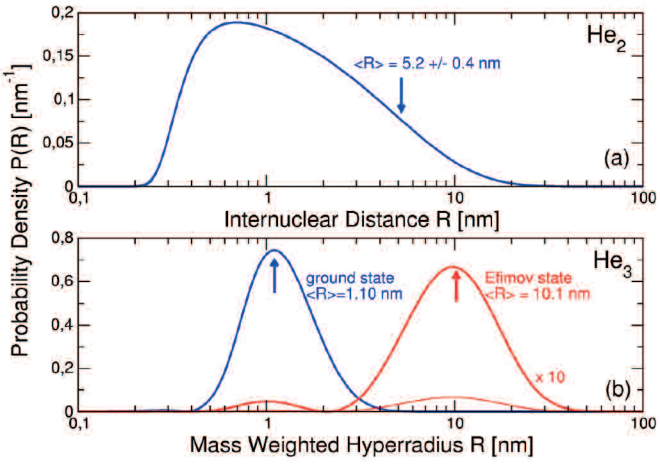

▲ **Fig. 4:** (a) Schematic diagram showing the probability density of the 1 S halo state of the He dimer and (b) The first excited Efimov and ground state of the He trimer as a function of an effective hyperspherical radius. The average radius of the dimer <R> = 5.2 ± 0.4 nm is more than 3 times larger than the classical outer turning point R_{out} = 1.4 nm of the interatomic potential (not shown). The first excited Efimov state of the trimer is even larger.

Indirect evidence for the existence of an Efimov state in magnetically tuned laser cooled 10 nK Cs gas has recently been reported [12].

Unexpected Magic He Cluster Sizes

In subsequent experiments the angular resolution was improved from $80 \cdot 10^{-6}$ to $20 \cdot 10^{-6}$. This made it possible to single out clusters with up to about 20 atoms. At diffraction angles less than $5 \cdot 10^{-4}$ *rad* corresponding to larger clusters a disturbing background from the large intensity of He atoms in the beam was eliminated by adjusting the mass spectrometer to He_2^+, to provide a measure of only the clusters in the beam. These experiments revealed a series of well-defined peaks, shown in Fig.5(a), which suggested the presence of stable magic cluster sizes [13]. This came as quite a surprise since the early calculations by nuclear theoreticians had repeatedly ruled out any exceptional magic number stabilities in ^{4}He clusters.

To analyze the unexpected features in the intensities they were transformed to obtain the underlying cluster size distributions G(N) shown in Fig.5(b) for the three diffraction patterns in Fig.5(a). The same features are seen in all three G(N) distributions even though the diffraction patterns appear to be quite different. The undulatory features modulate the exponential-like fall-off as emphasized by taking the ratio to the smoothed •••

▼ **Table 1:** Some Exceptionally Large Two-body Systems

Species	Size of constituent[m]	Distance between constituents [m]	Binding energy [eV]	Potential depth [eV]	Lifetime [sec]	Ref.
Deuteron	$\sim 8 \cdot 10^{-16}$	$4.3 \cdot 10^{-15}$	$2.2 \cdot 10^{6}$	$25 \cdot 10^{6}$	∞	-
He_2 ($\nu = 0$)	$\sim 10^{-10}$	$52 \cdot 10^{-10}$	$9.5 \cdot 10^{-8}$	$9.4 \cdot 10^{-4}$	∞	[7]
Na_2 $X^1\Sigma_g^+$ ($\nu = 65$)	$\sim 2 \cdot 10^{-10}$	$30\text{-}100 \cdot 10^{-10}$	$1.2 \cdot 10^{-5}$	0.69	∞	[9]
He_2^* O_u^+ ($\nu = 0\text{-}5$)	$\approx 3\text{-}5 \cdot 10^{-10}$	$100\text{-}800 \cdot 10^{-10}$	...	$8 \cdot 10^{-6}$	$\geq 10^{-8}$	[10]

··· fall-off (Fig.5(c)). This G(N) distribution is in itself of great interest since it represents the first unambiguous measurement of the size distribution of neutral clusters produced in a free jet expansion. The results have made it possible to test theories of homogeneous nucleation in much greater detail than previously possible.

Since all the total energy calculations rule out beyond a doubt any magic stabilities for ^{4}He clusters we had to look for another explanation for these unexpected features. Fortunately at that time Jesus Navarro and Rafael Guardiola (Valencia) had succeeded in applying the Diffusion Monte Carlo technique to the calculation of the excited cluster states. Their results for the entire range of sizes up to N = 50 are shown in Fig.6(a), where they are superimposed on the calculated chemical potential (the energy needed to detach one atom) $\mu(N) = \frac{\Delta E(N)}{\Delta N}$ [13], where $E(N)$ is the total internal energy. Then it became clear that the magic numbers found in our experiments correlated with those specific sizes at which a cluster acquires an additional bound state.

In order to understand how the addition of a bound state can affect the intensities it is necessary to consider in detail where the clusters stop growing in the expansion. Downstream of the orifice the rapidly decreasing density quickly drops below a value sufficient to maintain thermodynamic equilibrium. This point is called the "sudden freeze" distance and beyond this "point of no-return" the clusters no longer undergo collisions. Thus to a good approximation the cluster concentrations are determined by the equilibrium constant at the sudden freeze distance. Generally it is assumed that the growth of large clusters can be described by simple accretion: $He_{(N-1)} + He \rightarrow He_N$. The equilibrium constant K(N) for this reaction is given by the ratio of partition functions, Z, for a cluster with N atoms to that with N - 1 atoms. If the Nth cluster acquires an additional bound state its partition function will differ significantly from that for the next smaller N - 1 cluster and K(N) will jump in size. But for the next N + 1 cluster both Z_{N+1} and Z_N will have the same number of bound states and K(N+1) will fall back to a value close to that for N - 1 (Fig. 6(b)). The jumps in the ratios Z_N/Z_{N+1} agree nicely with the magic numbers in Fig.5(c).

Thus the observed magic numbers $\mathcal{N}$ are not at all related to the cluster stabilities, but have a new kinetic origin. These experiments confirm both the accuracy of the elementary excitation levels, as well as of the chemical potential. Finally it is interesting to point out that the energy levels in Fig.6(a) deviate significantly from those expected from the standard liquid drop model developed for nuclei. If the "soft" radial density distribution function of the clusters and a decrease in the surface tension with decreasing number of atoms is accounted for then, indeed, a correspondingly modified liquid drop model is consistent with the results. It is intriguing to note that this combined theory-experiment investigation sheds insight into the internal states of small clusters, which are expected to be superfluid [3]. These discrete states are the finite size forerunners of the famous bulk phonon-maxon-roton dispersion curve, predicted by Landau, which provides the microscopic basis for understanding many superfluid phenomena in the bulk. ■

About the Authors

Oleg Kornilov is currently setting up a femtosecond soft x-ray facility as a post-doc in the Lawrence Berkeley National Laboratory, University of California at Berkeley. He did his Ph.D research in Göttingen (2004) under the direction of **J. Peter Toennies**, who is an emeritus director at the Max Planck Institut für Dynamik und Selbstorganisation (formerly MPI für Strömungsforschung). At present he is especially interested in superfluidity in hydrogen clusters

Acknowledgments

For their important contributions to the success of these experiments we thank Rüdiger Brühl, Robert Grisenti, Anton Kalinin and Jens Pick. We also gratefully acknowledge the theoretical support from our Göttingen colleagues Gerhard C. Hegerfeldt, Thorsten Köhler and Martin Stoll as well as Jesus Navarro and Rafael Guardiola, both from Valencia. We thank Hartmut Hotop suggesting that we write this article and several valuable discussions.

References

[1] F. Dalfovo, S. Giorgini, L. P. Pitaevskii, and S. Stringari, *Rev. Mod. Phys.*, **71**, 463 (1999)

[2] W. Schöllkopf and J. P. Toennies, *Science* **266**, 1345 (1994)

[3] S. Grebenev, J. P. Toennies and A. F. Vilesov, *Science* **279**, 2083 (1998)

[4] Kalinin, O. Kornilov, W. Schöllkopf, and J. P. Toennies, *Phys. Rev. Lett.* **95**, 113402 (2005)

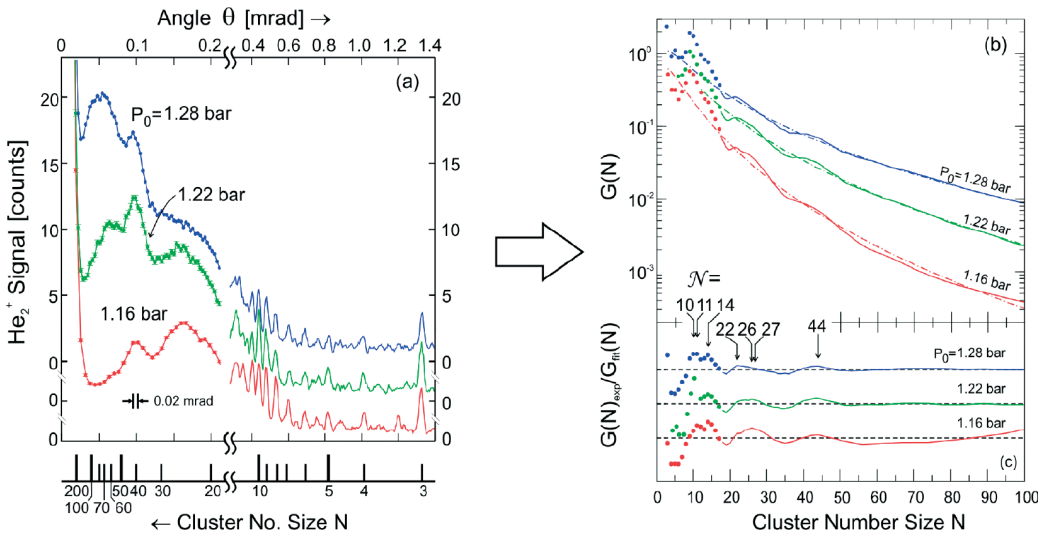

▶ **Fig. 5:** **(a)** Three typical diffraction patterns measured at high resolution for $T_0 = 6.7$ K and source pressures of $P_0 =$ 1.28 bar, 1.22 bar and 1.16 bar. **(b)** The size distributions G(N) obtained from a deconvolution of the raw data in (a) are plotted as a function of cluster number size N. **(c)** The curves in (b) have been divided by the average slope to emphasize the deviations. The maxima are assigned to the magic numbers $\mathcal{N}$ indicated by arrows in (c).

[5] R. E. Grisenti, W. Schöllkopf, J. P. Toennies, G. C. Hegerfeldt, and T. Köhler, *Phys. Rev. Lett.* **83**, 1755 (1999); J. D. Perreault, A. D. Cronin and T. A. Savas, *Phys. Rev.* **A71** 053612 (2005)

[6] R. Brühl, F. Fouquet, E. Grisenti, J. P. Toennies and G. C. Hegerfeldt, T. Köhler, M. Stoll, and Ch. Walter, *Europhys. Lett.* **59**, 357 - 363 (2002); J. C. Karam, N. Wipf, J. Grucker, F. Perales, M. Boustimi, G. Vassilev, V. Bocvarski, C. Mainos, J. Baudon, and J. Robert, *J. Phys. B: At. Mol. Opt. Phys.* **38**, 269 (2005)

[7] R. E. Grisenti, W. Schöllkopf, J. P. Toennies, G. C. Hegerfeldt, T. Köhler, and M. Stoll, *Phys. Rev. Lett.* **85**, 2284 (2000). Previously Gentry and colleagues measured the size of the dimer in a transmission experiment to be $\langle R \rangle = 6.2 \pm 1.0$ *nm* consistent with our value. [F. Luo, C. F. Giese, and W. R. Gentry, *J. Chem. Phys.* **104** (3), 1151 (1996)]

[8] A. Kalinin, O. Kornilov, L. Rusin, J. P. Toennies, and G. Vladimirov, *Phys. Rev. Lett.* **93**, 163402 (2004)

[9] P. D. Lett., P. S. Julienne, and W. D. Philipps, *Ann. Rev. Phys. Chem.* **46**, 423 (1995)

[10] J. Léonard, A. P. Mosk, M. Walhout, P. van der Straten, M. Leduc, and C. Cohen-Tannoudji, *Phys. Rev. A* **69**, 032702 (2004)

[11] R. Brühl, A. Kalinin, O. Kornilov, J. P. Toennies, G. C. Hegerfeldt, and M. Stoll, *Phys. Rev. Lett.* **95**, 063002 (2005)

[12] T. Kraemer, M. Mark, P. Waldburger, J. G. Danzl, C. Chin, B. Engeser, A. D. Lange, K. Pilch, A. Jaakkola, H.-C. Nägerl, and R. Grimm, *Nature*, **440**, 315 (2006)

[13] R. Brühl, R. Guardiola, A. Kalinin, O. Kornilov, J. Navarro, T. Savas, and J. P. Toennies, *Phys. Rev. Lett.* **92**, 185301 (2004); See also *J. Chem. Phys.* **124**, 084307-1 (2006)

[14] L. Hackermüller, S. Uttenthaler, K. Hornberger, E. Reiger, B. Brezger, A. Zeilinger, and M. Arndt, *Phys. Rev. Lett.* **91**, 090408 (2003)

[15] R. J. Glauber, *Phys. Rev.* **100**, 242 (1955)

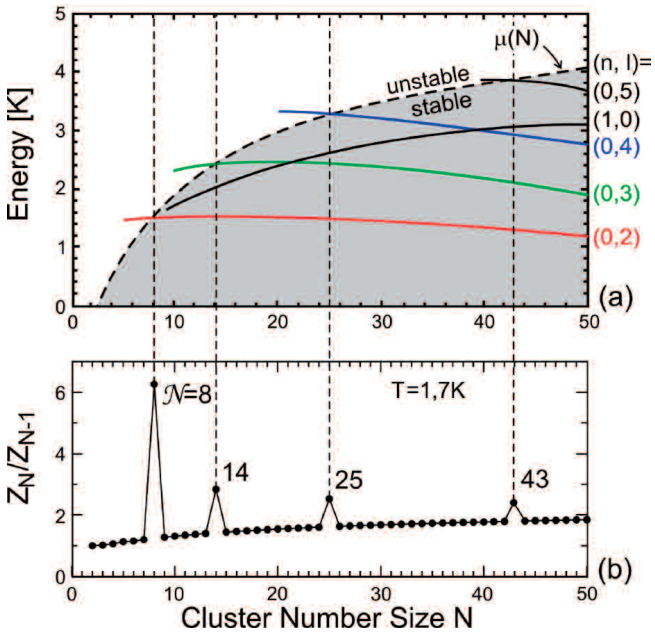

▲ **Fig. 6:** (a) The energies E(nl) of the collective excitations for different values of the radial and angular momentum quantum numbers (n,l) and the chemical potential (energy needed to evaporate one atom) are plotted as a function of N. (b) The ratio of the partition functions Z_n/Z_{N-1} is plotted versus N for an assumed cluster sudden freeze temperature of T = 1.7 K. At the threshold values in (a) the ratios show maxima, which explain the observed magic numbers N. The distorted spheres at the top illustrate the shapes of the clusters corresponding to each of the newly bound states.